fluids

MDPI

Article

Intra-Cardiac Kinetic Energy and Ventricular Flow Analysis in Bicuspid Aortic Valve: Impact on Left Ventricular Function, Dilation Severity, and Surgical Referral

Ali Fatehi Hassanabad [1] and Julio Garcia [2,3,4,5,6,*]

[1] Section of Cardiac Surgery, Department of Cardiac Science, University of Calgary, Calgary, AB T2N 1N4, Canada; ali.fatehihassanabad@albertahealthservices.ca
[2] Stephenson Cardiac Imaging Centre, University of Calgary, Calgary, AB T2N 1N4, Canada
[3] Department of Cardiac Sciences, Cumming School of Medicine, University of Calgary, Calgary, AB T2N 1N4, Canada
[4] Department of Radiology, Cumming School of Medicine, University of Calgary, Calgary, AB T2N 1N4, Canada
[5] Libin Cardiovascular Institute, University of Calgary, Calgary, AB T2N 1N4, Canada
[6] Alberta Children's Hospital Research Institute, University of Calgary, Calgary, AB T2N 1N4, Canada
* Correspondence: julio.garciaflores@ucalgary.ca

Abstract: Intra-cardiac kinetic energy (KE) and ventricular flow analysis (VFA), as derived from 4D-flow MRI, can be used to understand the physiological burden placed on the left ventricle (LV) due to bicuspid aortic valve (BAV). Our hypothesis was that the KE of each VFA component would impact the surgical referral outcome depending on LV function decrement, BAV phenotype, and aortic dilation severity. A total of 11 healthy controls and 49 BAV patients were recruited. All subjects underwent cardiac magnetic resonance imaging (MRI) examination. The LV mass was inferior in the controls than in the BAV patients (90 ± 26 g vs. 45 ± 17 g, $p = 0.025$), as well as the inferior ascending aorta diameter indexed (15.8 ± 2.5 mm/m^2 vs. 19.3 ± 3.5 mm/m^2, $p = 0.005$). The VFA KE was higher in the BAV group; significant increments were found for the maximum KE and mean KE in the VFA components ($p < 0.05$). A total of 14 BAV subjects underwent surgery after the scans. When comparing BAV nonsurgery vs. surgery-referred cohorts, the maximum KE and mean KE were elevated ($p < 0.05$). The maximum and mean KE were also associated with surgical referral (r = 0.438, $p = 0.002$ and r = 0.371, $p = 0.009$, respectively). In conclusion, the KE from VFA components significantly increased in BAV patients, including in BAV patients undergoing surgery.

Keywords: 4D-flow MRI; bicuspid aortic valve; ventricular flow analysis; kinetic energy

check for updates

Academic Editors: Xing Zhang and Eduardo Divo

Received: 2 October 2024
Revised: 12 December 2024
Accepted: 25 December 2024
Published: 27 December 2024

Citation: Fatehi Hassanabad, A.; Garcia, J. Intra-Cardiac Kinetic Energy and Ventricular Flow Analysis in Bicuspid Aortic Valve: Impact on Left Ventricular Function, Dilation Severity, and Surgical Referral. *Fluids* **2025**, *10*, 5. https://doi.org/10.3390/fluids10010005

Copyright: © 2024 by the authors. Licensee MDPI, Basel, Switzerland. This article is an open access article distributed under the terms and conditions of the Creative Commons Attribution (CC BY) license (https://creativecommons.org/licenses/by/4.0/).

1. Introduction

The aortic valve is one of four intra-cardiac valves that allows for forward blood flow to the body during each cardiac cycle. Normally, the aortic valve comprises three cusps, each opening and closing in synchrony to ensure systemic circulation is not compromised. Broadly, aortic valve disease can be acquired or be congenital [1]. Bicuspid aortic valve (BAV) is the most common congenital valvular abnormality, affecting 1–2% of the general population [2]. BAV affects flow patterns and dynamics so patients are at increased risk for developing bicuspid aortopathy, which refers to a dilated aorta [3]. Irregular flow patterns are believed to contribute to bicuspid aortopathy, a disease that is most often managed surgically [4]. Moreover, BAV has implications for intra-cardiac flow distribution, kinetic energy (KE), and pressure drop [5,6]. Cardiac magnetic resonance imaging (CMR) plays

an important role in the diagnosis of patients with BAV and abnormal flow patterns [2]. Particularly, four-dimensional-flow cardiac magnetic resonance imaging (4D-flow MRI) has been instrumental in accurately assessing blood hemodynamics, flow patterns, and flow energetics in patients with cardiovascular pathologies, including BAV [2,7–10].

Blood flow through the left ventricle (LV), which may be influenced by a BAV phenotype, can be an important marker of LV function. Intra-cardiac KE is also a novel and non-invasive metric that can be used to determine LV function [11–15]. Ventricular flow assessment (VFA) using 4D-flow MRI characterizes LV blood flow distribution using four functional components: direct flow (DF), retained inflow (RI), delayed ejection (DE), and residual volume (RV) [5,16–19]. Long intra-cardiac KE of each one of these components can provide the individual energy expended during the cardiac cycle. Callaghan et al. objectively quantified VFA after surgical intervention and revealed that disordered ventricular flow patterns are associated with blood-flow viscous energy losses [20]. Recently, our group used 4D-flow MRI to accurately visualize and quantify the blood flow reliability of VFA and pressure drops in BAV patients with preserved ejection fraction (pEF) [5]. That study was novel in showing that VFA is not sensitive in differentiating BAV patients with mild regurgitation from healthy controls with pEF because VFA components and EF are global parameters. Inversely, pressure (local measurement) may be a more reliable biomarker to reveal the early stage of diastolic dysfunction. Nevertheless, the role of the KE of each VFA component as a marker for LV impairment prior to surgery has remained unexplored.

The purpose of this study is to assess the KE contribution of each VFA component in patients with BAV. We hypothesized that the KE of each VFA component would impact the surgical referral outcome depending on LV function decrement, BAV phenotype, and aortic dilation severity. This study may provide important insight into the extent to which VFA components may drive differences in KE in patients with BAV. Our findings may be used to better understand how intra-cardiac hemodynamics are affected by BAV before surgery.

2. Materials and Methods

2.1. Study Cohort

A total of 60 subjects, including 11 healthy volunteer controls (age = 32 $\pm$ 14 years, 7 female) and 49 BAV patients (age = 45 $\pm$ 17 years, 14 female), were recruited as part of a pre-defined prospective observational sub-study of the Cardiovascular Imaging Registry of Calgary (CIROC, NCT04367220). Patients enrolled between March 2017 and August 2022 were considered for this study. All subjects provided written informed consent. The Conjoint Health Research Ethics Board approved this study at the University of Calgary (REB#13-0902). All research procedures were performed in agreement with the Declaration of Helsinki. This study was coordinated by commercial software (cardioDI™ v2024.0.0; Cohesic Inc., Calgary, AB, Canada) for the routine capture of patient informed consent and health questionnaires and for the standardized collection of MRI-related variables. The patients were distinguished by standardized coding of clinical referral indications for BAV, including BAV morphology characterization. Only cases with a research 4D-flow MRI acquisition were considered for this study. The exclusion criteria for the patients included a history of myocardial infarction, non-ischemic cardiomyopathy, complex congenital heart disease, MRI-coded moderate–severe mitral valve insufficiency, and significant systolic dysfunction [left ventricle ejection fraction (LVEF) < 50%]. Healthy volunteers of $\geq$17 years of age were recruited and underwent identical workflow and were required to have no known cardiovascular disease, hypertension, or diabetes and have no contraindications for MRI [21]. No age or sex matching between the BAV patients and controls was considered.

2.2. Cardiac Magnetic Resonance Acquisition

All study participants underwent a standardized cardiac imaging protocol using 3T MRI scanners (Skyra, Prisma, Siemens, Erlangen, Germany). We had optimized this protocol for BAV assessment as reported in [5,6,22,23]. Multi-planar segmented, ECG-gated, time-resolved balanced steady-state free precession (SSFP) cine imaging in 4-chamber, 3-chamber, 2-chamber, and short-axis views were achieved, covering the whole heart at end-expiration for functional assessment of the LV. For volumetric assessment, 3D magnetic resonance angiography (MRA) of the whole heart was acquired by administrating 0.2 mmol/kg gadolinium contrast (Gadovist, Bayer, Mississauga, ON, Canada). At approximately 5–10 min following contrast administration, retrospective ECG-gated 4D-flow MRI (WIP 785A) was acquired during free-breathing using navigator gating of diaphragmatic motion, Figure 1a, as described in previous studies [5,6,23]. Velocity encoding selection was based on standard 2D flow measurements in the aorta and a 3-chamber scout to avoid aliasing. The temporal resolution range was given by patients' ECG cycle durations fitting the standard 30 frames of acquisition. The 4D-flow MRI parameters were as follows: spatial resolution (2.0–2.5 mm × 2.0–2.5 mm × 2.5–3.5 mm), temporal resolution (36–40 ms), flip angle (15°), velocity encoding (150–550 cm/s), echo time (2.01–2.35 ms), and repetition time (4.53–5.07 ms). The scan times ranged from 8 to 12 min depending on physiological factors, pre-defined scanner parameters, and respiratory gating efficiency.

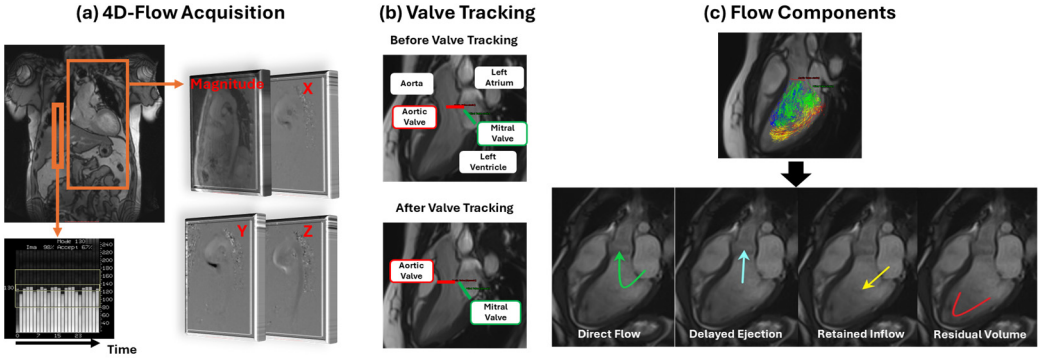


Figure 1. Acquisition and analysis of 4D-flow MRI. (**a**) Acquisition planning of 4D-flow MRI requires a respiratory navigator and whole-heart coverage using sagittal planes. (**b**) Valve tracking of the aortic and mitral valves requires standard three-chamber acquisitions for automated detection and tracking of the valves. A co-registration to the 4D-flow volume facilitates with plane location for flow component analysis. (**c**) Illustration of the visualization of intra-cardiac pathlines used for the assessment of ventricular flow analysis and its corresponding components.

2.3. Cardiac Magnetic Resonance Imaging and 4D-Flow Analysis

All analyses were completed by a single observer using cvi[42] v5.17 (Circle Cardiovascular Imaging Inc., Calgary, Canada). We derived the functional parameters of LVs from cardiac MR images, as described in [5]. Briefly, LV end-systolic volume (LVESV) and left ventricular end-diastolic volume (LVEDV) were obtained and indexed to the body surface area (BSA). The cvi[42] prototype 4D-flow module was used to analyze the LV flow components during a cardiac cycle. This prototype version allowed the calculation of KE on each VFA component, as given by $KE = \frac{1}{2}\rho \cdot V \cdot v^2$, assuming a blood density of 1.06 g/mL (ρ), the volume of a voxel (V), and the velocity magnitude (v). Standard corrections for phase-offset, static tissue, and velocity aliasing were performed when necessary. Most of the preprocessing was automated, and it is given by the following steps: (1) data cropping to the region of interest using a bounding-box mask; (2) velocity preprocessing, including automated offset correction based on a static tissue and vessel mask that can be adjusted using a threshold; and (3) anti-aliasing correction (up to 2 times the velocity encoding). In

this 4D-flow module version, no LV segmentation was required for the VFA. Automated detection of the aortic (AV) and mitral valve (MV) location and motion was performed using machine learning in a 3-chamber view and constrained to the 4D-flow volume [24]. Briefly, it starts with selecting the long-axis three-chamber SSFP cine image to localize the AV and MV planes on each frame. In the three-chamber cine views, tissue feature tracking was applied to turn the initial static planes to dynamic according to the valve motion during each cardiac cycle [24]. This approach demonstrated excellent inter- and intra-observer variability [24]. Color-coded flow visualization was used for detailed semiautomatic locating and contouring of AVs and MVs. This approach allowed us to properly delineate the annulus of the AV and MV. Our single analyst modified the valves' locations when it was necessary for precise contouring of the 4D-flow images throughout the cardiac cycle. The isovolumetric relaxation phase was identified for the VFA.

The intra-cardiac LV blood flow was divided into four components over the cardiac cycle: Figure 1c shows (I) direct flow (DF), the blood volume that enters and leaves the LV during the same cardiac cycle; (II) retained inflow (RI), the blood volume that enters the LV during the diastolic phase and does not eject in the systolic phase in the same cardiac cycle; (III) delayed ejection (DE) flow, the blood volume retained in the LV and ejected in the next systole; and (IV) residual volume (RV), the amount of blood that remains in the LV for two cardiac cycles or more. The LV flow component analysis is described in full detail in [5,19]. The isovolumetric relaxation (IVR) phase was set where both the AV and MV flow profiles were minimized (both valves were closed) at the end of the systolic phase. The four components of the left ventricular flow (DF, DE, RI, and RV) were acquired according to a previously accredited method [25,26]. The VFA methodology was initially validated by Eriksson et al. in a small cohort of subjects [25]. In addition, Stoll et al. conducted test–retest variability validation [27]. Pathline particles were emitted from each voxel within the LV chamber and separated into four flow components along with the corresponding KE. Statistical analysis was conducted using SPSS version 29 (IBM, Chicago, IL, USA) and included power calculation for group comparison as recommended by Eng [28], a normality test based on Kolmogorov–Smirnov and Shapiro–Wilk, group comparison between controls and BAV patients, surgery vs. nonsurgery referral, and valve type phenotype comparison (Type 0, Type 1 RN, and Type 1 RL) that was performed based on distribution type using Student's t-test or the Mann-Whitney U-test for multiple-comparison one-way ANOVA with post hoc pairwise comparison and the Bonferroni correction when appropriate. Associations between the VFA, KE, LV function and surgery referral were performed using Pearson's correlation. Effect size was evaluated using Cohen's d. p-values of <0.05 were considered significant.

3. Results

3.1. Cohort Characteristics

The total sample size estimation for the VFA was 12 subjects, and for the KE, it was 15 subjects. Sixty participants were enrolled in this study; 11 were healthy and 49 were patients with BAV. Counting the BAV phenotype classes revealed 16 cases of Type 0, 31 cases of Type 1 and 2 cases of Type 2. The healthy control group was significantly younger than the BAV group (32 $\pm$ 14 vs. 45 $\pm$ 17, p = 0.005). Sixty-four percent of the healthy cohort was females compared with 29% in the BAV group, which was also significant (p = 0.029). Compared to the BAV subjects, the healthy participants had significantly lower BSAs (1.77 $\pm$ 0.24 m^2 vs. 1.98 $\pm$ 0.23 m^2, p = 0.010). Comorbidities and medications were only reported in patients with BAV. A total of 24 patients reported alcohol consumption occasionally (12%) or regularly (37%). Based on BMI, a total of 8 patients as opposed to 49 were reported with obesity. For medications, 18% of the BAV patients were taking

beta blockers, 24% ACIi/ARB, and 16% statins. With respect to the LV parameters, the LV masses indexed were lower in the controls than the BAV patients (52 ± 10 g/m^2 vs. 63 ± 21 g/m^2, p = 0.002). The indexed ascending aorta (AAo) diameter of the healthy control group was significantly less than that of the BAV patients (15.8 ± 2.5 mm/m^2 vs. 19.3 ± 3.5 mm/m^2, p =0.005). The study cohort characteristics are summarized in Table 1.

Table 1. Baseline characteristics.

Parameter	Control (n = 11)	BAV (n = 49)	*p*-Value
Age (years)	32 ± 14	45 ± 17	0.005
Sex, n female (%)	7 (64)	14 (29)	0.029
BSA (m^2)	1.77 ± 0.24	1.98 ± 0.23	0.010
Cigarette smoking n (%)		8 (16%)	
Alcohol consumption n (%)			
None		25 (51%)	
Occasional (<1 drink/day)		6 (12%)	
Regular (>1 drink/day)		18 (37%)	
Diabetes mellitus n (%)		-	
Hypertension n (%)		2 (4%)	
Dyslipidemia n (%)		1 (2%)	
Hypothyroidism n (%)		-	
Chronic kidney disease n (%)		-	
Atrial fibrillation n (%)			
Paroxysmal		1 (2%)	
Persistent		-	
Dyspnea (NYHA class ≥ II) n (%)		-	
Obesity n (%)		8 (16%)	
Medications			
Aspirin n (%)		3 (6%)	
Beta blockers n (%)		9 (18%)	
ACIi/ARB n (%)		12 (24%)	
Calcium channel blocker n (%)		-	
Anti-coagulant n (%)		3 (6%)	
Loop diuretic n (%)		-	
Statin n (%)		8 (16%)	
CMR			
LVEDVi (mL/m^2)	87 ± 16	94 ± 24	0.083
LVESVi (mL/m^2)	33 ± 9	38 ± 14	0.086
LVEF (%)	63 ± 6	60 ± 11	0.308
LV mass indexed (g/m^2)	52 ± 10	63 ± 21	0.002
AAo diameter indexed (mm/m^2)	15.8 ± 2.5	19.3 ± 3.5	0.005

AAo: ascending aorta; ACIi/ARB: angiotensin-converting enzyme inhibitor/angiotensin receptor blocker; BSA: body surface area; CMR: cardiac magnetic resonance; LVEDVi: left ventricular end-diastolic volume indexed; LVESVi: left ventricular end-systolic volume indexed; LVEF: Left Ventricular Ejection Fraction; NYHA: New York Heart Association.

3.2. Ventricular Flow Component Quantification

With respect to the ventricular flow components, there were significant differences ($p < 0.05$) in the residual volume (RV), the maximum residual volume kinetic energy (KE RV Max), the mean of the delayed ejection flow kinetic energy (KE DE Mean), and the mean of the residual volume kinetic energy (KE RV Mean). Except for the DF, the parameters were higher in the BAV group compared to the healthy control participants. Semiautomated contouring required minimal adjustment of the AVs during diastole in 8 cases, and the MVs required plane adjustments in 1 case and early systolic adjustments in 5 cases. The quantifications of the ventricular flow components are summarized in Table 2.

Table 2. Ventricular flow components.

Parameter	Control (n = 11)	BAV (n = 49)	*p*-Value	Cohen's d
DF (%)	32 (27, 37)	26 (25, 30)	0.135	0.446
DE (%)	25 (24, 30)	23 (23, 26)	0.134	0.453
RI (%)	22 (18, 23)	19 (17, 20)	0.106	0.484
RV (%)	22 (16, 26)	28 (27, 32)	0.003	−0.964
KE DF Max (μJ)	2336 (1637, 3189)	2688 (2606, 3528)	0.339	−0.405
KE DE Max (μJ)	1907 (1220, 2480)	2216 (2347, 3721)	0.178	−0.506
KE RI Max (μJ)	1094 (641, 1293)	1178 (1243, 1805)	0.166	−0.577
KE RV Max (μJ)	304 (179, 469)	628 (725, 1297)	0.016	−0.713
KE DF Mean (μJ)	682 (476, 903)	785 (742, 1034)	0.225	−0.391
KE DE Mean (μJ)	450 (312, 577)	595 (585, 1028)	0.048	−0.483
KE RI Mean (μJ)	273 (167, 323)	338 (323, 481)	0.080	−0.583
KE RV Mean (μJ)	115 (71, 195)	245 (276, 495)	0.006	−0.685

Data are presented as medians (25th percentile, 75th percentile). DF: direct flow; DE: delayed ejection flow; RI: retained inflow; RV: residual volume; KE: kinetic energy; Max: maximum.

3.3. Patients with BAV Undergoing Surgery

A total of 14 of the 49 BAV subjects underwent surgery after their MRI examination. Table 3 summarize baseline characteristics of nonsurgical and surgical patients. The surgical patients were older than the nonsurgical patients, with a non-significant age difference. Only 3 opposed to 14 female patients underwent surgical treatment. Severe aortic stenosis and severe aortic dilation were the main reasons for surgery. Surgical referral included two aortic repairs, 9 valve replacements, and three for both aortic repair and valve replacement. When comparing the BAV nonsurgery vs. surgery-referred cohorts, the indexed aortic diameter was significantly higher (18.4 ± 2.9 mm/m^2 vs. 22.1 ± 3.5 mm/m^2, $p < 0.001$), and the maximum KE in the RV (500 μJ (494 μJ, 964 μJ) vs. 1618 μJ (1022 μJ, 2614 μJ), $p = 0.013$, d = −1.16) and the mean KE in the RV (210 μJ (208 μJ, 378 μJ) vs. 403 μJ (313 μJ, 986 μJ), $p = 0.032$, d = −0.961) were similarly elevated. No differences were found in the KE for the BAV phenotype.

Table 3. Baseline characteristics of nonsurgical and surgical patients.

Parameter	Nonsurgical (n = 35)	Surgical (n = 14)	*p*-Value
Age (years)	44 ± 17	50 ± 14	0.28
Sex, n female (%)	11 (31)	3 (21)	0.356
BSA (m^2)	2.00 ± 0.25	1.97 ± 0.19	0.676
Aortic stenosis			
Mild n (%)	4 (11)	1 (7)	
Moderate n (%)	2 (6)	3 (21)	
Severe n (%)	0 (0)	4 (29)	
Aortic regurgitation			
Mild n (%)	6 (17)	4 (29)	
Moderate n (%)	2 (6)	0 (0)	
Severe n (%)	0 (0)	1 (7)	
Aortic dilation			
Mild n (%)	4 (11)	3 (21)	
Moderate n (%)	6 (17)	1 (7)	
Severe n (%)	1 (3)	3 (21)	
Surgical referral			
Aortic repair n (%)		2	

Table 3. *Cont.*

Parameter	Nonsurgical (n = 35)	Surgical (n = 14)	*p*-Value
Valve replacement n (%)		9	
Aortic repair and valve replacement n (%)		3	
CMR			
LVEDVi (mL/m^2)	89 ± 19	104 ± 29	0.059
LVESVi (mL/m^2)	37 ± 12	40 ± 17	0.502
LVEF (%)	59 ± 11	63 ± 7	0.207
LV mass indexed (g/m^2)	59 ± 15	71 ± 30	0.081
AAo diameter indexed (mm/m^2)	18.4 ± 2.9	22.1 ± 3.5	<0.001

BSA: body surface area; CMR: cardiac magnetic resonance; LVEDVi: left ventricular end-diastolic volume indexed; LVESVi: left ventricular end-systolic volume indexed; LVEF: Left Ventricular Ejection Fraction.

3.4. Ventricular Flow Component Associations

The DF correlated with the LVESVi (r = −0.256, p = 0.048), and the DE correlated with the LVEDVi (r = 0.385, p = 0.02), LVESVi (r = 0.545, p < 0.001), and LVEF (r = −0.323, p = 0.029). The maximum KE of the DF, DE, and RI correlated with the LVEDVi (r = 0.317, p = 0.014; r = 0.518, p < 0.001, Figure 2a; and r = 0.289, p = 0.025, respectively). The maximum KE of the DE and RI correlated with the LVESVi (r = 0.447, p < 0.001, Figure 2b; r = 0.313, p = 0.015, respectively). Only the maximum KE of the RV correlated with the LV masses indexed (r = 0.368, p = 0.004). The correlations of the mean KE of the DF, DE, RI, and RV with LVEDVi are presented in Figure 3. The correlations of the mean KE of the DF, DE, RI, and RV with the LVESVi are presented in Figure 4. The maximum and mean RV KE were also associated with surgical referral (r = 0.438, p = 0.002; and r = 0.371, p = 0.009; respectively).

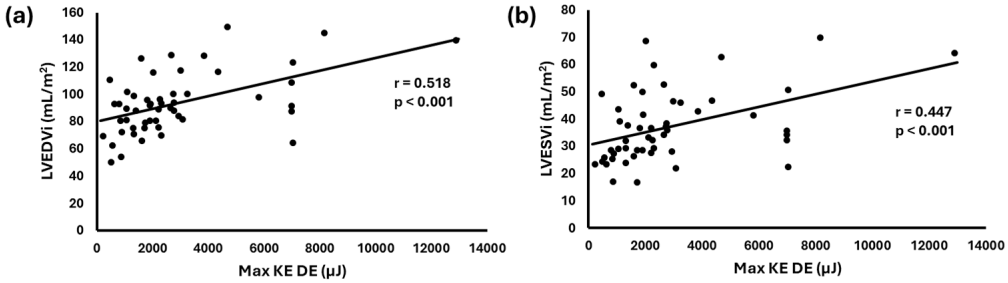


Figure 2. Correlation of maximum kinetic energy for delayed ejection (Max KE DE). LVEDVi: left ventricular end-diastolic volume indexed; LVESVi: left ventricular end-systolic volume indexed.

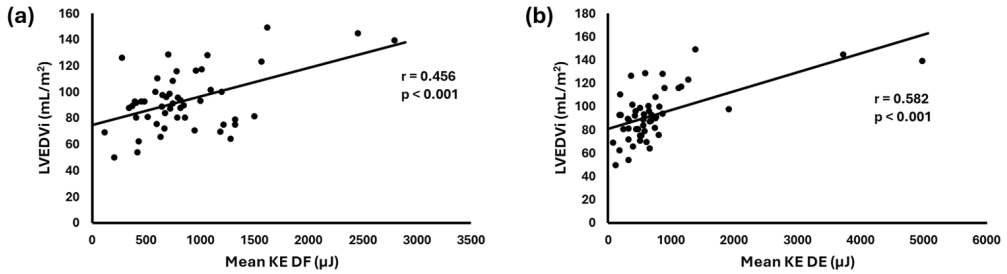


Figure 3. *Cont.*

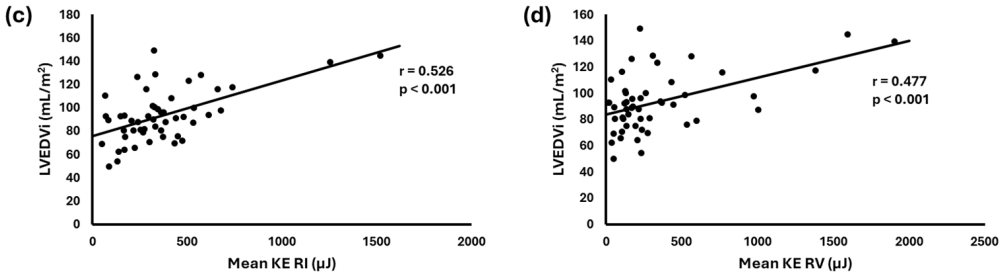


Figure 3. Correlations of mean kinetic energy (KE) for ventricular flow components with left ventricular end-diastolic volume indexed (LVEDVi). (**a**) Scatter plot showing the correlation of mean KE from direct flow (DF) and LVEDVi; (**b**) Scatter plot showing the correlation of mean KE from delayed ejection flow (DE) and LVEDVi; (**c**) Scatter plot showing the correlation of mean KE from retained inflow (RI) and LVEDVi; (**d**) Scatter plot showing the correlation of mean KE from residual volume (RV) and LVEDVi.

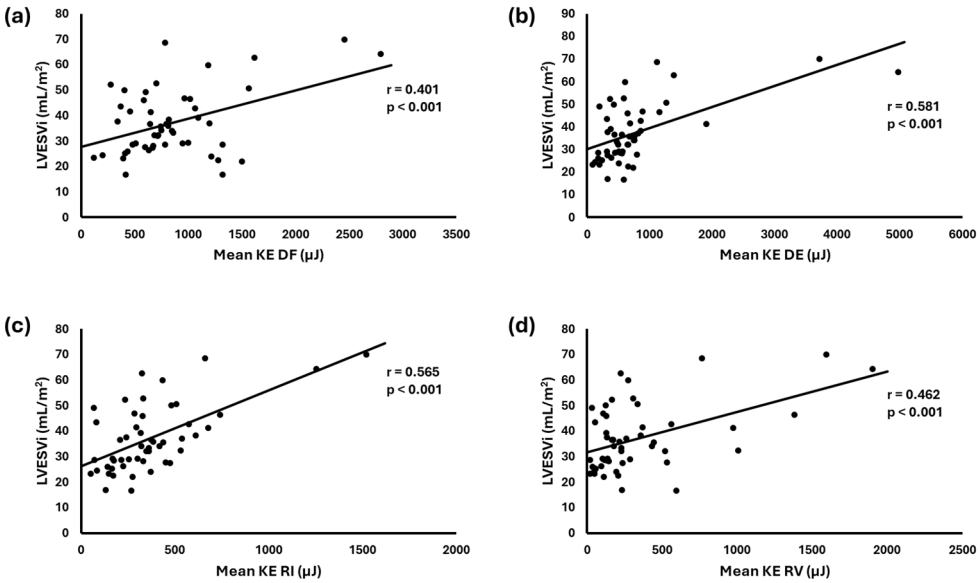


Figure 4. Correlations of mean kinetic energy (KE) for ventricular flow components with left ventricular end-systolic volume indexed (LVESVi). (**a**) Scatter plot showing the correlation of mean KE from direct flow (DF) and LVESVi; (**b**) Scatter plot showing the correlation of mean KE from delayed ejection flow (DE) and LVESVi; (**c**) Scatter plot showing the correlation of mean KE from retained inflow (RI) and LVESVi; (**d**) Scatter plot showing the correlation of mean KE from residual volume (RV) and LVESVi.

4. Discussion

This study demonstrated that cardiac magnetic resonance imaging can identify LV hemodynamic differences via VFA components and kinetic energy in BAV patients beyond the standard metrics. We showed that VFA components, which can be quantified non-invasively, may be important for the assessment of BAV for three main reasons. First, the VFA components and energetics can be accurately quantified. Second, there are differences between patients with BAV and healthy subjects. Third, compared to nonsurgical patients, patients with BAV who undergo surgery have significant differences in a subset of VFA components.

Accurate quantification of valvular disease is essential for optimal clinical management. Using 4D-flow MRI, analysis planes can be applied and modified according to the location and angulation of moving valvular structures for the quantification of valvular regurgitation, while peak velocity quantification of stenotic jets can be performed to elucidate valvular stenoses. Moreover, an important part of the total work of the heart transfers into

the KE of the blood, where the KE is directly involved in the movement of the blood [29]. These metrics have been shown to have clinical relevance. Our study included younger controls than BAV patients. A study from Zhao et al. reported that VFA components may not be sensitive to age [30]. However, LV KE is affected by age [30,31]. Similarly, biological sex was not balanced in our study, and it has been reported that females may present higher LV KE than males [30,31]. Age and sex matching may be important aspects to consider in future studies with BAV. Differences in BSA between the controls and patients were an anticipated finding. No relevant impact of BSA was reported for the VFA and LV KE at the time of data analysis. Another expected finding was the difference in the LV parameters between the controls and the patients with BAV. Limited knowledge was found for assessing VFA and LV KE in BAV. However, few studies have investigated LV KE in other cardiovascular diseases. Eriksson and colleagues found that patients with heart failure and mild LV remodeling exhibited impaired preservation of inflow KE compared to healthy individuals despite equivalent stroke volumes [32]. Furthermore, the total direct flow KE at end-diastole was lower in heart failure patients, which may have impacted diastolic–systolic coupling. Another study demonstrated that myocardial infarction was associated with a decrease in average LV KE over the whole cardiac cycle [11]. Additionally, 4D-flow MRI quantification of LV flow components and energetics may also provide a consistent classification for impaired LV filling. For instance, Crandon et al. showed that in healthy individuals, LV KE during E and A waves presented a stronger relation with increasing age than 2D mitral inflow measurements [33]. Another study, which investigated right and left atrial KE in healthy volunteers, found three peaks in the KE time profiles in both atria: during the ventricular systole, the early ventricular diastole, and atrial contraction [34]. The early diastolic KE of the LA correlated with the LV mass, whereas such an association was not noted in the right chambers. Based on more recent studies, LV mass seems to play an important role in increasing the pressure gradient within the LV during the diastole [35].

In the present study, for the first time, we considered intra-cardiac flow components and their KE in patients with BAV. Importantly, we ascertained that differences exist in specific metrics in patients with BAV compared to healthy controls. Efficient blood flow transportation in the LV is associated with DF [36]. In our study, the BAV DF was reduced but not significantly when compared with the controls. The VFA RV component and its KE were the unique parameters that consistently detected differences between the control and BAV groups. These findings may be due to the increased load in the LVs of BAV patients. Furthermore, in a sub-population analysis, we found that specific VFA components can differ in BAV patients undergoing surgical intervention versus those not requiring operations. In our study, the AAo diameter was higher in the BAV patients compared to the controls. As the severity of BAV increases, affecting aortic dilation and LV function, the blood flow KE is expected to increase along the dilation of the aorta and at the time of surgery [6,37]. Overall, the understanding of the role of LV intra-cardiac KE in BAV is limited in clinical settings. LV KE is expected to change with increased LV load due to the severity of the BAV. Our KE results aligned with this expectation. The latter may be critical in the clinical setting, as it facilitates a non-invasive approach to better delineate surgical decision-making and provide potential insight into clinical outcomes. A recent study from Elhawaz et al. piloted the usefulness of LV KE and VFA in aortic stenosis intervention [38]. They found that LV KE and VFA components significantly changed ($p < 0.05$) after intervention. Interestingly, pre-operative LV KE was associated with LV remodeling post-intervention. Our study can be the foundation for future work, which should focus on determining whether the timing of pre-operative imaging can affect ventricular flow assessment and if there is any impact on clinical outcomes. Furthermore, Carlsson et al. demonstrated that LV KE can increase by ~20%

during exercise in healthy controls [39]. Exercise stress 4D-flow imaging in valvular disease, especially BAV, remains unexplored but may have added value for assessing LV viability before surgery. However, recent studies have reported that in congenital diseases, LV KE can significantly increase during exercise [40–42]. Predictive models, based on LV KE and VFA, differentiating surgical outcomes across different BAV phenotypes may be determinant for personalized surgical planning. A more advanced approach could include the use of physical twins mapping the disease states of patients to KE measurements and predictive surgical models [43]. For the latter, a large longitudinal sample size may be required.

This study has limitations that should be acknowledged. This study would have benefitted from a larger sample size, allowing us to better differentiate BAV phenotypes, aortopathy dilation patterns, and LV remodeling patterns. There were only 14 females in the BAV cohort, which limited the understanding of KE in female BAV patients. Future studies should include more females to better elucidate whether sex can make a difference in intra-cardiac VFA components in BAV patients. All the participants and scans were from one center, using only one type of 4D-flow sequence and a single reader and reviewer. The latter is important considering the manual corrections performed in the AV and MV contouring. A multicenter study can aid in establishing the external validity of this study by including multiple scanner vendors and 4D-flow sequence types. The BAV phenotype classes were unbalanced, with Type 2 having only 2 cases, limiting the statistical test for BAV phenotyping. It must also be considered that, as with any advanced 4D-flow derived metric, spatial and temporal resolution may have affected the accuracy of the KE. Our 4D-flow protocol followed the recommendations of the 4D-flow consensus, and small modifications to spatial resolution were determined by patient comfort at the time of examination [44–46]. In our study, we did not consider any additional validation for VFA and KE. Doppler vector mapping could be an option for 2D KE validation [47], but it may have limitations for 3D assessment. Alternatively, an in silico validation could be possible by extracting the LV volume and valve morphology from MRI examination. AV and MV 4D-flow measurements may serve as initialization for a simulation. An additional consideration is that our subjects were not sex-and age matched, which may be required to consider in future studies. Lastly, our sample size estimation was mostly based on VFA components and mean LV KE in consideration of the high sensitivity of maximum LV KE. The latter may require further investigation, considering that LV KE data derived from VFA components in BAV are limited and additional experimental data are required.

5. Conclusions

In this study, we showed that KE from VFA components is increased in patients with BAV and in BAV patients undergoing surgery. Moreover, KE is associated with ventricular function and surgical referral. These findings may be useful to characterize energetic changes in BAV due to LV remodeling and surgical therapy and aid in delivering precise therapeutic strategies that can be personalized.

Author Contributions: Conceptualization, J.G.; methodology, J.G.; software, J.G.; validation, J.G. and A.F.H.; formal analysis, J.G. and A.F.H.; investigation, J.G. and A.F.H.; resources, J.G.; data curation, J.G.; writing—original draft preparation, A.F.H. and J.G.; writing—review and editing, J.G.; visualization, J.G.; supervision, J.G.; project administration, J.G.; funding acquisition, J.G. All authors have read and agreed to the published version of the manuscript.

Funding: This research was funded by The University of Calgary; J.G. start-up funding (#11022618 and #11021988). We acknowledge the support of the Natural Science and Engineering Research Council of Canada/Conseil de recherche en science naturelles et en génie du Canada, RGPIN-2020-04549 and DGECR-2020-00204. NSERC Alliance—Alberta Innovates Advance Program (#232403115).

Data Availability Statement: The anonymized data are available upon request from the corresponding author.

Acknowledgments: The authors thank all investigators, clinical staff, and participants of the Cardiovascular Imaging Registry of Calgary (CIROC) for their valuable contributions.

Conflicts of Interest: The authors declare that this research was conducted without any commercial or financial relationships that could be constructed as potential conflicts of interest.

References

1. Isselbacher, E.M.; Preventza, O.; Hamilton Black, J.; Augoustides, J.G.; Beck, A.W.; Bolen, M.A.; Braverman, A.C.; Bray, B.E.; Brown-Zimmerman, M.M.; Chen, E.P.; et al. 2022 ACC/AHA Guideline for the Diagnosis and Management of Aortic Disease: A Report of the American Heart Association/American College of Cardiology Joint Committee on Clinical Practice Guidelines. *Circulation* **2022**, *146*, E334–E482. [CrossRef]
2. Fatehi Hassanabad, A.; King, M.A.; Di Martino, E.; Fedak, P.W.M.; Garcia, J. Clinical implications of the biomechanics of bicuspid aortic valve and bicuspid aortopathy. *Front. Cardiovasc. Med.* **2022**, *9*, 922353. [CrossRef]
3. Verma, S.; Siu, S.C. Aortic dilatation in patients with bicuspid aortic valve. *N. Engl. J. Med.* **2014**, *370*, 1920–1929. [CrossRef]
4. Borger, M.A.; Fedak, P.W.M.M.; Stephens, E.H.; Gleason, T.G.; Girdauskas, E.; Ikonomidis, J.S.; Khoynezhad, A.; Siu, S.C.; Verma, S.; Hope, M.D.; et al. The American Association for Thoracic Surgery consensus guidelines on bicuspid aortic valve–related aortopathy: Full online-only version. *J. Thorac. Cardiovasc. Surg.* **2018**, *156*, e41–e74. [CrossRef]
5. Aliabadi, S.; Sojoudi, A.; Bandali, M.F.; Bristow, M.S.; Lydell, C.; Fedak, P.W.M.; White, J.A.; Garcia, J. Intra-cardiac pressure drop and flow distribution of bicuspid aortic valve disease in preserved ejection fraction. *Front. Cardiovasc. Med.* **2022**, *9*, 903277. [CrossRef]
6. Geeraert, P.; Jamalidinan, F.; Burns, F.; Jarvis, K.; Bristow, M.S.; Lydell, C.; Hidalgo Tobon, S.S.; de Celis Alonso, B.; Fedak, P.W.M.; White, J.A.; et al. Hemodynamic Assessment in Bicuspid Aortic Valve Disease and Aortic Dilation: New Insights From Voxel-By-Voxel Analysis of Reverse Flow, Stasis, and Energetics. *Front. Bioeng. Biotechnol.* **2022**, *9*, 725113. [CrossRef]
7. Qin, J.J.; Indja, B.; Gholipour, A.; Gök, M.; Grieve, S.M. Evaluation of Left Ventricular Function Using Four-Dimensional Flow Cardiovascular Magnetic Resonance: A Systematic Review. *J. Cardiovasc. Dev. Dis.* **2022**, *9*, 304. [CrossRef] [PubMed]
8. Gorecka, M.; Bissell, M.M.; Higgins, D.M.; Garg, P.; Plein, S.; Greenwood, J.P. Rationale and clinical applications of 4D flow cardiovascular magnetic resonance in assessment of valvular heart disease: A comprehensive review. *J. Cardiovasc. Magn. Reson.* **2022**, *24*, 49. [CrossRef]
9. Ashkir, Z.; Myerson, S.; Neubauer, S.; Carlhäll, C.-J.; Ebbers, T.; Raman, B. Four-dimensional flow cardiac magnetic resonance assessment of left ventricular diastolic function. *Front. Cardiovasc. Med.* **2022**, *9*, 866131. [CrossRef]
10. Hassanabad, A.F.; Garcia, J.; Verma, S.; White, J.A.J.A.; Fedak, P.W.M. Utilizing wall shear stress as a clinical biomarker for bicuspid valve-associated aortopathy. *Curr. Opin. Cardiol.* **2019**, *34*, 124–131. [CrossRef]
11. Garg, P.; Crandon, S.; Swoboda, P.P.; Fent, G.J.; Foley, J.R.J.; Chew, P.G.; Brown, L.A.E.; Vijayan, S.; Hassell, M.E.C.J.; Nijveldt, R.; et al. Left ventricular blood flow kinetic energy after myocardial infarction—Insights from 4D flow cardiovascular magnetic resonance. *J. Cardiovasc. Magn. Reson.* **2018**, *20*, 61. [CrossRef] [PubMed]
12. Frank, S.; Lee, J.; Lantz, J.; Ebbers, T.; Shadden, S.C. Cardiac Kinetic Energy and Viscous Dissipation Rate From Radial Flow Data. *Front. Physiol.* **2021**, *12*, 725104. [CrossRef] [PubMed]
13. Jeong, D.; Anagnostopoulos, P.V.; Roldan-Alzate, A.; Srinivasan, S.; Schiebler, M.L.; Wieben, O.; François, C.J. Ventricular kinetic energy may provide a novel noninvasive way to assess ventricular performance in patients with repaired tetralogy of Fallot. *J. Thorac. Cardiovasc. Surg.* **2015**, *149*, 1339–1347. [CrossRef]
14. Demirkiran, A.; van Ooij, P.; Westenberg, J.J.M.; Hofman, M.B.M.; van Assen, H.C.; Schoonmade, L.J.; Asim, U.; Blanken, C.P.S.; Nederveen, A.J.; van Rossum, A.C.; et al. Clinical intra-cardiac 4D flow CMR: Acquisition, analysis, and clinical applications. *Eur. Heart J. Cardiovasc. Imaging* **2022**, *23*, 154–165. [CrossRef] [PubMed]
15. Wong, J.; Chabiniok, R.; Tibby, S.M.; Pushparajah, K.; Sammut, E.; Celermajer, D.; Giese, D.; Hussain, T.; Greil, G.F.; Schaeffter, T.; et al. Exploring kinetic energy as a new marker of cardiac function in the single ventricle circulation. *J. Appl. Physiol.* **2018**, *125*, 889–900. [CrossRef]
16. Demirkiran, A.; van der Geest, R.J.; Hopman, L.H.G.A.; Robbers, L.F.H.J.; Handoko, M.L.; Nijveldt, R.; Greenwood, J.P.; Plein, S.; Garg, P. Association of left ventricular flow energetics with remodeling after myocardial infarction: New hemodynamic insights for left ventricular remodeling. *Int. J. Cardiol.* **2022**, *367*, 105–114. [CrossRef]
17. Demirkiran, A.; Hassell, M.E.C.J.; Garg, P.; Elbaz, M.S.M.; Delewi, R.; Greenwood, J.P.; Piek, J.J.; Plein, S.; van der Geest, R.J.; Nijveldt, R. Left ventricular four-dimensional blood flow distribution, energetics, and vorticity in chronic myocardial infarction patients with/without left ventricular thrombus. *Eur. J. Radiol.* **2022**, *150*, 110233. [CrossRef] [PubMed]

18. Kaur, H.; Assadi, H.; Alabed, S.; Cameron, D.; Vassiliou, V.S.; Westenberg, J.J.M.; van der Geest, R.; Zhong, L.; Dastidar, A.; Swift, A.J.; et al. Left Ventricular Blood Flow Kinetic Energy Assessment by 4D Flow Cardiovascular Magnetic Resonance: A Systematic Review of the Clinical Relevance. *J. Cardiovasc. Dev. Dis.* **2020**, *7*, 37. [CrossRef]
19. Kim, H.; Sheitt, H.; Wilton, S.B.; White, J.A.; Garcia, J. Left Ventricular Flow Distribution as a Novel Flow Biomarker in Atrial Fibrillation. *Front. Bioeng. Biotechnol.* **2021**, *9*, 725121. [CrossRef]
20. Callaghan, F.M.; Burkhardt, B.; Valsangiacomo Buechel, E.R.; Kellenberger, C.J.; Geiger, J. Assessment of ventricular flow dynamics by 4D-flow MRI in patients following surgical repair of d-transposition of the great arteries. *Eur. Radiol.* **2021**, *31*, 7231–7241. [CrossRef]
21. Kramer, C.M.; Barkhausen, J.; Bucciarelli-Ducci, C.; Flamm, S.D.; Kim, R.J.; Nagel, E. Standardized cardiovascular magnetic resonance imaging (CMR) protocols: 2020 update. *J. Cardiovasc. Magn. Reson.* **2020**, *22*, 17. [CrossRef]
22. Nightingale, M.; Scott, M.B.; Sigaeva, T.; Guzzardi, D.; Garcia, J.; Malaisrie, S.C.; McCarthy, P.; Markl, M.; Fedak, P.W.M.; Di Martino, E.S.; et al. Magnetic resonance imaging-based hemodynamic wall shear stress alters aortic wall tissue biomechanics in bicuspid aortic valve patients. *J. Thorac. Cardiovasc. Surg.* **2023**, *168*, 465–476.e5. [CrossRef]
23. Geeraert, P.; Jamalidinan, F.; Fatehi Hassanabad, A.; Sojoudi, A.; Bristow, M.; Lydell, C.; Fedak, P.W.M.; White, J.A.; Garcia, J. Bicuspid aortic valve disease is associated with abnormal wall shear stress, viscous energy loss, and pressure drop within the ascending thoracic aorta: A cross-sectional study. *Medicine* **2021**, *100*, e26518. [CrossRef]
24. Garcia, J.; Beckie, K.; Hassanabad, A.F.; Sojoudi, A.; White, J.A. Aortic and mitral flow quantification using dynamic valve tracking and machine learning: Prospective study assessing static and dynamic plane repeatability, variability and agreement. *JRSM Cardiovasc. Dis.* **2021**, *10*, 204800402199990. [CrossRef] [PubMed]
25. Eriksson, J.; Carlhäll, C.J.; Dyverfeldt, P.; Engvall, J.; Bolger, A.F.; Ebbers, T. Semi-automatic quantification of 4D left ventricular blood flow. *J. Cardiovasc. Magn. Reson.* **2010**, *12*, 9. [CrossRef] [PubMed]
26. Eriksson, J.; Dyverfeldt, P.; Engvall, J.; Bolger, A.F.; Ebbers, T.; Carlhäll, C.J. Quantification of presystolic blood flow organization and energetics in the human left ventricle. *Am. J. Physiol. Heart Circ. Physiol.* **2011**, *300*, H2135–H2141. [CrossRef] [PubMed]
27. Stoll, V.M.; Loudon, M.; Eriksson, J.; Bissell, M.M.; Dyverfeldt, P.; Ebbers, T.; Myerson, S.G.; Neubauer, S.; Carlhäll, C.-J.; Hess, A.T. Test-retest variability of left ventricular 4D flow cardiovascular magnetic resonance measurements in healthy subjects. *J. Cardiovasc. Magn. Reson.* **2018**, *20*, 15. [CrossRef] [PubMed]
28. Eng, J. Sample size estimation: How many individuals should be studied? *Radiology* **2003**, *227*, 309–313. [CrossRef] [PubMed]
29. Prec, O.; Katz, L.N.; Sennett, L.; Rosenman, R.H.; Fishman, A.P.; Hwang, W. Determination of kinetic energy of the heart in man. *Am. J. Physiol. Content* **1949**, *159*, 483–491. [CrossRef]
30. Zhao, X.; Tan, R.-S.; Garg, P.; Chai, P.; Leng, S.; Bryant, J.A.; Teo, L.L.S.; Yeo, T.J.; Fortier, M.V.; Low, T.T.; et al. Age- and sex-specific reference values of biventricular flow components and kinetic energy by 4D flow cardiovascular magnetic resonance in healthy subjects. *J. Cardiovasc. Magn. Reson.* **2023**, *25*, 50. [CrossRef]
31. Zhao, X.; Tan, R.-S.; Garg, P.; Chai, P.; Leng, S.; Bryant, J.; Teo, L.L.S.; Ong, C.C.; van der Geest, R.J.; Allen, J.C.; et al. Impact of age, sex and ethnicity on intra-cardiac flow components and left ventricular kinetic energy derived from 4D flow CMR. *Int. J. Cardiol.* **2021**, *336*, 105–112. [CrossRef] [PubMed]
32. Eriksson, J.; Bolger, A.F.; Ebbers, T.; Carlhäll, C.-J. Four-dimensional blood flow-specific markers of LV dysfunction in dilated cardiomyopathy. *Eur. Heart J. Cardiovasc. Imaging* **2013**, *14*, 417–424. [CrossRef] [PubMed]
33. Crandon, S.; Westenberg, J.J.M.; Swoboda, P.P.; Fent, G.J.; Foley, J.R.J.; Chew, P.G.; Brown, L.A.E.; Saunderson, C.; Al-Mohammad, A.; Greenwood, J.P.; et al. Impact of Age and Diastolic Function on Novel, 4D flow CMR Biomarkers of Left Ventricular Blood Flow Kinetic Energy. *Sci. Rep.* **2018**, *8*, 14436. [CrossRef] [PubMed]
34. Arvidsson, P.M.; Töger, J.; Heiberg, E.; Carlsson, M.; Arheden, H. Quantification of left and right atrial kinetic energy using four-dimensional intracardiac magnetic resonance imaging flow measurements. *J. Appl. Physiol.* **2013**, *114*, 1472–1481. [CrossRef]
35. Steding-Ehrenborg, K.; Arvidsson, P.M.; Töger, J.; Rydberg, M.; Heiberg, E.; Carlsson, M.; Arheden, H. Determinants of kinetic energy of blood flow in the four-chambered heart in athletes and sedentary controls. *Am. J. Physiol. Circ. Physiol.* **2016**, *310*, H113–H122. [CrossRef] [PubMed]
36. van der Geest, R.J.; Garg, P. Advanced Analysis Techniques for Intra-cardiac Flow Evaluation from 4D Flow MRI. *Curr. Radiol. Rep.* **2016**, *4*, 38. [CrossRef]
37. Binter, C.; Gotschy, A.; Sündermann, S.H.; Frank, M.; Tanner, F.C.; Lüscher, T.F.; Manka, R.; Kozerke, S. Turbulent Kinetic Energy Assessed by Multipoint 4-Dimensional Flow Magnetic Resonance Imaging Provides Additional Information Relative to Echocardiography for the Determination of Aortic Stenosis Severity. *Circ. Cardiovasc. Imaging* **2017**, *10*, e005486. [CrossRef]
38. Elhawaz, A.; Archer, G.T.; Zafar, H.; Fidock, B.; Barker, N.; Jones, R.; Rothman, A.; Hose, R.; Al-Mohammad, A.; Briffa, N.; et al. Left ventricular blood flow kinetic energy is associated with the six-minute walk test and left ventricular remodelling post valvular intervention in aortic stenosis. *Quant. Imaging Med. Surg.* **2021**, *11*, 1470–1482. [CrossRef] [PubMed]

39. Carlsson, M.; Heiberg, E.; Toger, J.; Arheden, H. Quantification of left and right ventricular kinetic energy using four-dimensional intracardiac magnetic resonance imaging flow measurements. *Am. J. Physiol. Heart Circ. Physiol.* **2012**, *302*, H893–H900. [CrossRef] [PubMed]
40. Zhao, X.; Hu, L.; Leng, S.; Tan, R.-S.; Chai, P.; Bryant, J.A.; Teo, L.L.S.; Fortier, M.V.; Yeo, T.J.; Ouyang, R.Z.; et al. Ventricular flow analysis and its association with exertional capacity in repaired tetralogy of Fallot: 4D flow cardiovascular magnetic resonance study. *J. Cardiovasc. Magn. Reson.* **2022**, *24*, 4. [CrossRef] [PubMed]
41. Stöhr, E.J.; González-Alonso, J.; Bezodis, I.N.; Shave, R. Left ventricular energetics: New insight into the plasticity of regional contributions at rest and during exercise. *Am. J. Physiol. Circ. Physiol.* **2014**, *306*, H225–H232. [CrossRef] [PubMed]
42. Macdonald, J.A.; Roberts, G.S.; Corrado, P.A.; Beshish, A.G.; Haraldsdottir, K.; Barton, G.P.; Goss, K.N.; Eldridge, M.W.; Francois, C.J.; Wieben, O. Exercise-induced irregular right heart flow dynamics in adolescents and young adults born preterm. *J. Cardiovasc. Magn. Reson.* **2021**, *23*, 116. [CrossRef] [PubMed]
43. Sel, K.; Osman, D.; Zare, F.; Masoumi Shahrbabak, S.; Brattain, L.; Hahn, J.; Inan, O.T.; Mukkamala, R.; Palmer, J.; Paydarfar, D.; et al. Building Digital Twins for Cardiovascular Health: From Principles to Clinical Impact. *J. Am. Heart Assoc.* **2024**, *1*, e0319813. [CrossRef]
44. Bissell, M.M.; Raimondi, F.; Ait Ali, L.; Allen, B.D.; Barker, A.J.; Bolger, A.; Burris, N.; Carhäll, C.-J.; Collins, J.D.; Ebbers, T.; et al. 4D Flow cardiovascular magnetic resonance consensus statement: 2023 update. *J. Cardiovasc. Magn. Reson.* **2023**, *25*, 40. [CrossRef] [PubMed]
45. Zhong, L.; Schrauben, E.M.; Garcia, J.; Uribe, S.; Grieve, S.M.; Elbaz, M.S.M.; Barker, A.J.; Geiger, J.; Nordmeyer, S.; Marsden, A.; et al. Intracardiac 4D Flow MRI in Congenital Heart Disease: Recommendations on Behalf of the ISMRM Flow & Motion Study Group. *J. Magn. Reson. Imaging* **2019**, *50*, 677–681. [CrossRef]
46. Garcia, J.; Barker, A.J.A.J.; Markl, M. The Role of Imaging of Flow Patterns by 4D Flow MRI in Aortic Stenosis. *JACC Cardiovasc. Imaging* **2019**, *12*, 252–266. [CrossRef] [PubMed]
47. Vixège, F.; Berod, A.; Sun, Y.; Mendez, S.; Bernard, O.; Ducros, N.; Courand, P.-Y.; Nicoud, F.; Garcia, D. Physics-constrained intraventricular vector flow mapping by color Doppler. *Phys. Med. Biol.* **2021**, *66*, 245019. [CrossRef] [PubMed]

Disclaimer/Publisher's Note: The statements, opinions and data contained in all publications are solely those of the individual author(s) and contributor(s) and not of MDPI and/or the editor(s). MDPI and/or the editor(s) disclaim responsibility for any injury to people or property resulting from any ideas, methods, instructions or products referred to in the content.